Design, Synthesis, and Biological Evaluation of 6α- and 6β-*N*-Heterocyclic Substituted Naltrexamine Derivatives as μ Opioid Receptor Selective Antagonists

Guo Li,[†] Lindsey C. Aschenbach,[†] Jianyang Chen,[†,§] Michael P. Cassidy,[‡] David L. Stevens,[‡] Bichoy H. Gabra,[‡] Dana E. Selley,[‡] William L. Dewey,[‡] Richard B. Westkaemper,[†] and Yan Zhang[†,*]

Department of Medicinal Chemistry, Department of Pharmacology and Toxicology, Virginia Commonwealth University, 410 North 12th Street, P.O. Box 980540, Richmond, Virginia 23298-0540

Received October 7, 2008

Opioid receptor selective antagonists are important pharmacological probes in opioid receptor structural characterization and opioid agonist functional study. Thus far, a nonpeptidyl, highly selective and reversible μ opioid receptor (MOR) antagonist is unavailable. On the basis of our modeling studies, a series of novel naltrexamine derivatives have been designed and synthesized. Among them, two compounds were identified as leads based on the results of in vitro and in vivo assays. Both of them displayed high binding affinity for the MOR (K_i = 0.37 and 0.55 nM). Compound **6** (NAP) showed over 700-fold selectivity for the MOR over the δ receptor (DOR) and more than 150-fold selectivity over the κ receptor (KOR). Compound **9** (NAQ) showed over 200-fold selectivity for the MOR over the DOR and approximately 50-fold selectivity over the KOR. Thus these two novel ligands will serve as leads to further develop more potent and selective antagonists for the MOR.

Introduction

Opioid antagonists have played very important roles in the study of opioid receptors. In fact, the action of an agonist is characterized as opioid-receptor-mediated only if it is competitively antagonized by an opioid antagonist.[1,2] Receptor-selective opioid antagonists are important tools to identify the receptor types that mediate the effects of opioid agonists.[3] The characterization of the μ opioid receptor (MOR[a]) is essential because the analgesic function and addiction/abuse liability of many clinically available opiates are primarily due to their interaction with the MOR.[1,2,4] Thus, MOR selective antagonists are essential for the study of MOR function in drug abuse and addiction. In fact, some antagonists with relatively low selectivity for MOR, e.g., naltrexone, have been shown to inhibit relapse and curb drug craving in opiate addicts.[5−7]

On the basis of the "message-address concept", highly selective nonpeptide antagonists for the κ opioid receptor (e.g., norbinaltorphimine (norBNI) and 5′-guanidinonaltrindole (GNTI))[8,9] and for the δ receptor (e.g., naltrindole (NTI))[10] (Figure 1) were designed and synthesized several years ago. These compounds are widely used as selective ligands in pharmacological studies.

Thus far, however, no optimal nonpeptide antagonist has been developed for the MOR, although some moderately potent ligands, e.g., cyprodime,[11] are available. Compared with the high selectivity of GNTI for the κ opioid receptor (KOR) (K_i values ratios are $\mu/\kappa \approx 120$, $\delta/\kappa \approx 250$)[9] and NTI for the δ opioid receptor (DOR) (K_i values ratios are $\mu/\delta \approx 152$, $\kappa/\delta \approx 276$),[10] cyprodime only has a moderate selectivity of the MOR over the DOR and KOR (K_i values ratios are $\kappa/\mu \approx 45$, $\delta/\mu \approx 40$).[12] Another drawback of cyprodime is that it has much lower affinity for the MOR than naloxone and naltrexone,[11] which limits its utility. Further structure−activity relationship studies of cyprodime derivatives did not generate any additional antagonist with significantly improved affinity or selectivity for the MOR.[13−17] Although β-funaltrexamine (β-FNA), clocinnamox, and others (Figure 2) have been reported as selective and irreversible nonpeptide antagonists for MOR,[18−21] the fact that they bind covalently with the receptor largely limits their utility. In most cases, a reversible antagonist would be preferred because it can inhibit the receptors temporarily for pharmacological study and then can be washed out from the binding locus to "revive" the receptors afterward.

Most highly selective and reversible μ opioid receptor antagonists currently available are conformation-constrained peptides, e.g., CTOP and CTAP.[22−28] They are relatively metabolically stable and have been used to target the MOR in in vitro and in vivo studies while their limited bioavailability may not be suitable for many types of in vivo studies and for medical applications. Optimal utility of antagonists as pharmacological tools requires both in vitro and in vivo activity. Nonpeptide ligands are preferred due to their ability to penetrate the CNS and lesser vulnerability to metabolic inactivation compared to the peptide agents. Therefore, the development of a nonpeptide, potent, selective, and reversible antagonist for the μ opioid receptor is highly desirable.

Naltrexone is a promising template for the design of the opioid receptor selective ligands. The successful modification of naltrexone in the synthesis of NTI, norBNI, and GNTI are good examples. While naltrexone has nanomolar affinity for all three opioid receptors, it also shows moderate selectivity for the MOR over DOR and KOR. Some chemical structure features are essential for its high affinity for the opioid receptors and should not be abolished. For example, the addition of a 3-hydroxyl group onto cyprodime and its derivatives will

* To whom correspondence should be addressed. Phone: 804-828-0021. Fax: 804-828-7625. E-mail: yzhang2@vcu.edu.

† Department of Medicinal Chemistry, Virginia Commonwealth University.

‡ Department of Pharmacology and Toxicology, Virginia Commonwealth University.

§ Current address: Zhejiang Jingxin Pharmaceutical Co. Ltd., 800 Eastern Dadao Road, Xinchang County, Zhejiang Province, China 312500.

[a] Abbreviations: GPCRs, G-protein coupled receptors; MOR, μ opioid receptor; DOR, δ opioid rececptor; KOR, κ opioid receptor; norBNI, norbinaltorphimine; GNTI, 5′-guanidinonaltrindole; NTI, naltrindole; β-FNA, β-funaltrexamine; EL, extracellular loop; NTX, naltrexone; CHO, Chinese hamster ovarian.

10.1021/jm801272c CCC: $40.75
Published on Web 02/06/2009

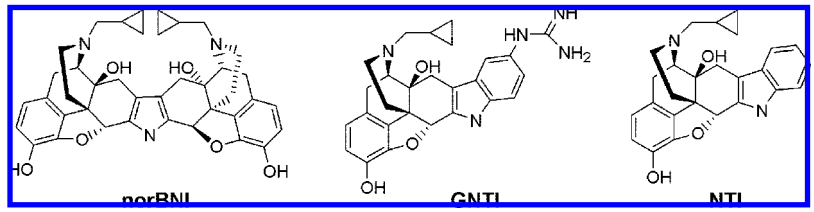

Figure 1. The κ opioid receptor selective antagonist norBNI, GNTI, and the δ opioid receptor selective antagonist NTI.

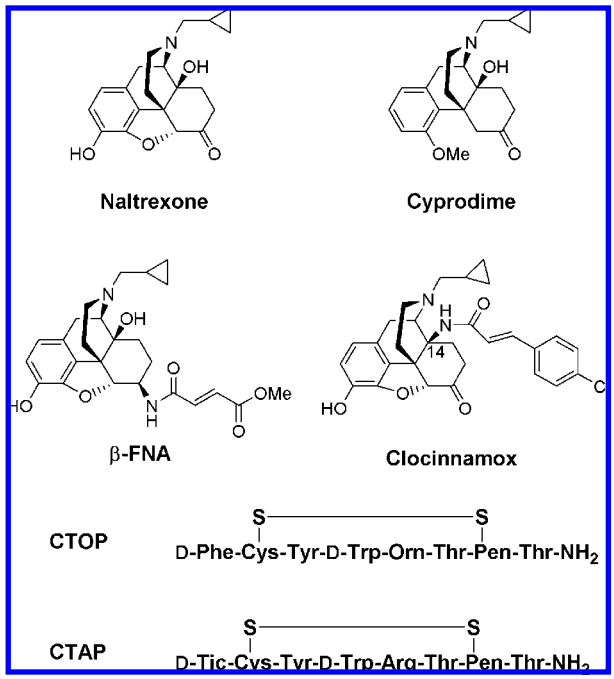

Figure 2. The μ opioid receptor selective antagonists.

"markedly enhance affinity at all three opioid receptors".[13] In addition, the chemistry related to the structural modification of naltrexone has been thoroughly studied. This information will be beneficial to the synthetic route design of naltrexone derivatives.

In this paper, we report the design, synthesis, and biological evaluation of two series of novel naltrexone-derived ligands as selective MOR antagonists. Molecular modeling of the naltrexone binding pocket in the homology models of the three opioid receptors led to the identification of an alternative "address" domain in the MOR that may enhance selectivity for the MOR over the DOR and KOR. Two series of ligands were designed and synthesized as proof-of-concept. Biological evaluation of these two series of compounds revealed some ligands with high affinity and selectivity for the MOR. On the basis of these results, two lead compounds have been identified for future optimization.

Results and Discussion

Molecular Modeling. To facilitate ligand design, homology models of all three opioid receptors were constructed. To date, in the whole superfamily of G-protein coupled receptors (GPCRs), only the X-ray crystal structures of bovine rhodopsin,[29−32] opsin,[33] and the human β2- and β1-adrenergic receptor[34−38] have been successfully obtained with high resolution. Most molecular models of other GPCRs have been constructed using the rhodopsin structure as a template. Therefore, homology models of the μ, δ, and κ opioid receptors were constructed based on the X-ray crystal structure of bovine rhodopsin after sequence alignment (Figure 3). Molecular dynamics simulations were conducted to optimize the conformation of the models. The models contain not only the transmembrane helices but also the extracellular and intracellular domains so that these models were integrated and complete. The MOR model was also optimized in a membrane−aqueous system.[39] The DOR and KOR models were also optimized following the same method. All amino acid residues in these three models have reasonable bond lengths and bond angles. The analysis of φ, Ψ, χ_1, and χ_2 angles of the resulting protein conformations was further conducted with Procheck 4.1 (see Supporting Information).

Because naltrexone is a universal antagonist at all three opioid receptors with moderate selectivity for the MOR, we decided to use it as a probe molecule to identify the antagonist binding site in all three opioid receptors. By comparison of the differences among these three binding pockets, we attempted to identify the amino acid residues that are critical to ligand selectivity for the MOR. Three steps were involved in the identification of the critical amino acid residues that differentiate the binding affinity of naltrexone in the three opioid receptors. The first step was the interactive docking of naltrexone into the binding locus of the receptor to form the ligand−receptor complex. The second step was energy minimization and molecular dynamics carried out for the ligand−receptor system to relax and optimize binding interactions between the ligand and amino acid residues in the binding cavity. The third step is the identification and comparison of the naltrexone binding locus in all the three receptors. The ligand−receptor complex structure obtained after 11 ps of molecular dynamics simulation is depicted in Figure 4. In these complexes, the distance between the protonated nitrogen atom in the 17-amino group of NTX and the carboxyl group of Asp147 (D3.32) was initially anchored at 4.0 Å and retained at this value by a weak harmonic restraint (2 kcal/Å) during the molecular dynamics simulation to represent the putative salt bridge that has been inferred from experimental studies.[53] In the lowest energy conformation of the complex extracted from the last 5 ps molecular dynamics simulation, the distance (4.1 Å) was compatible with the initial setting.

As shown in Figure 4A, in the binding pocket of naltrexone, the entire molecule in the MOR was mainly composed of aliphatic amino acid residues. The positively charged amino moiety of the ligand was within the range of an ionic interaction with Asp147 (D3.32). We also noticed that the carbonyl group on C(6) of naltrexone was orienting toward an aromatic binding pocket formed mainly by amino acid residues from the extracellular loops (ELs) of the receptor, including Tyr210 (Yxl2.43) and Phe221 (Fxl2.54) from EL2 and Trp318 (W7.35) at the border of EL3 and Helix 7.

In Figure 4B, the naltrexone's binding pocket in the DOR was very similar to that in the MOR except that there existed no aromatic binding locus formed by multiple amino acid residues to which the C(6) carbonyl group of naltrexone pointed. At the conserved region, only Phe202 (Fxl2.54) from EL2 was in the vicinity while Pro191 (Pxl2.43) and Leu300 (L7.35) are

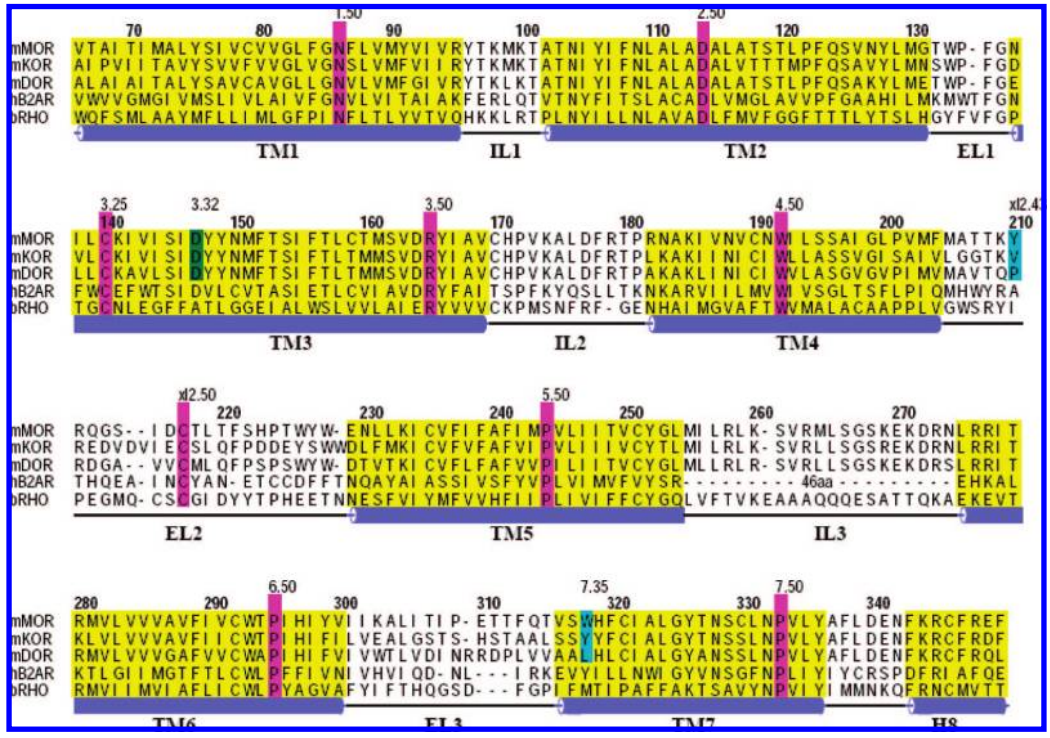

Figure 3. The sequence alignment of the MOR, DOR, and KOR with human β2AR and bovine rhodposin. The Ballesteros−Weinstein numbering system was adopted to mark all the conserved amino acid residues among most of the GPCRs and colored in red. The extracellular loop 2 (EL2) was numbered following the assignment proposed by Johnson et al.[61] The MOR protein was numbered accordingly above its sequence. The secondary structure of the MOR receptor 3D conformation based on bovine rhodopsin crystal structure was marked out below all the sequences. The conserved aspartate residues (D3.32) among all three opioid receptors were marked out in green. The two nonconserved residues xl2.43 and 7.35 were marked out in blue.

not aromatic ones. This difference might be applicable in the design of ligands that are selective for the MOR over the DOR.

Further study of the naltrexone binding pocket in the KOR (Figure 4C) showed that there was an aromatic/aliphatic binding pocket formed with the contribution of Phe214 (Fxl2.54) from EL2, Phe231 (F5.37) on helix 5, and Tyr313 (Y7.35) from helix 7. However, only one residue Tyr313 (Y7.35) may form a hydrogen bond with the ligand, while in the MOR binding locus, at least two of them are available to be considered.

Therefore, our molecular modeling study of the MOR antagonist binding pocket using naltrexone as the probe has revealed an aromatic binding locus at the extracellular loop region. Further comparison with the DOR and KOR antagonist binding pockets indicated that the existence of amino acid residues acting as potential hydrogen bonding donors and/or acceptors may be a unique structural feature of this aromatic binding locus in the MOR. Therefore, this binding domain may serve as an alternate "address" motif in the MOR that contributes to ligand recognition of the MOR selectively over DOR and KOR. Molecular design targeting to this "address" domain could lead to the identification of selective MOR antagonists. To be noticed, accumulated evidence has shown that the extracellular loops of GPCRs may play a critical role in the binding pocket of their small molecule ligands, including a number of opioid receptor agonists and antagonists.[39−46] It has been found that EL3 of the MOR is critical for the binding of MOR-selective agonists by comparing their binding affinities for MOR/DOR and MOR/KOR chimeric receptors with those for the wild-type MOR, DOR, and KOR.[43,44] Site-directed mutagenesis studies have revealed that certain amino acid residues in EL3 could be essential for ligand (including agonist and antagonist) selectivity for the MOR.[45−47] More specifically, Trp318 from EL3 has been identified as an important residue for the binding affinity and selectivity of varies ligands for the MOR.[40,41,43,48] These reports are consistent with the observation from our modeling studies.

Molecular Design. On the basis of the molecular modeling study, two series of ligands were designed as MOR selective antagonists (Table 1). None of them have been discussed in the literature as selective opioid receptor ligands.

In the structure of these ligands, we introduced a heteroaromatic moiety onto the 6-position of naltrexone. An amide bond was adopted as the linkage of the side chain moiety to the morphinan skeleton. Therefore, these ligands can be considered derivatives of naltrexamine. The configuration of C(6) will be either α or β. Such a stereochemical arrangement could play an important role for the affinity and the selectivity of the ligand, as has been demonstrated by β-FNA and α-FNA.[49] The aromatic character of this side chain was designed to have aromatic stacking interaction with the aromatic binding locus in the MOR in order to differentiate from the DOR. The nitrogen atom in the aromatic system will act as a hydrogen bond acceptor to probe for the potential formation of a hydrogen bond with Tyr210 or Trp318 in the binding locus from the ELs of the MOR in order to possibly differentiate from the KOR. Compounds with phenyl and naphthalenyl substitutions were designed as control compounds to test our hypothesis. These two series of ligands served as proof-of-concept to test the identification of the alternate "address" domain in MOR.

Chemical Synthesis. For the synthesis of these 6-substituted derivatives of naltrexamine, the starting material was naltrexone. The stereoselective synthesis of α- and β-naltrexamine has been applied successfully in the synthesis of their derivatives in the literature.[50]

In our case, α-naltrexamine was obtained with a yield of 60% in three steps, while β-naltrexamine was obtained with a yield of 63% in three steps. The amide bond formation between the

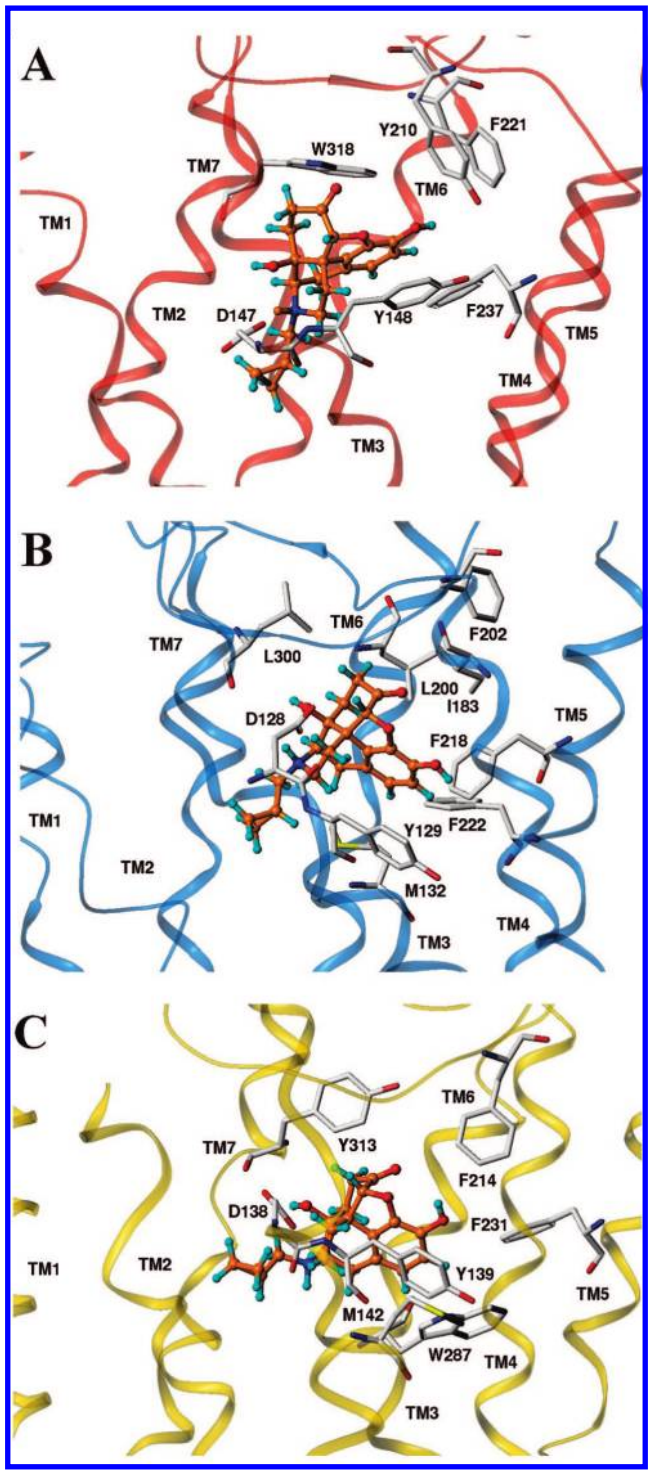

Figure 4. Naltrexone (NTX) docked in the homology models in the MOR, DOR, and KOR. NTX is in ball and stick, and colored as carbon, red-orange; hydrogen, cyan; oxygen, red and nitrogen, blue; the amino acid residues are in stick and colored as carbon, grey; oxygen, red and nitrogen, blue. The receptor homology models are in ribbon. NTX is in A) MOR, red; B) DOR, cyan; and C) KOR, yellow.

naltrexamine and the side chain moiety was straightforward. Depending on the commercial availability of the aromatic moiety, either in acyl chloride or acid form, condition 1 or 2 was adopted. Under mild basic condition, the intermediate, 3,6-disubstituted naltrexamine, was converted to the 6-monosubstituted target compound (Scheme 1) with reasonable yield. All the ligands were fully characterized before submitting for biological studies.

Biological Evaluation. Biological screening for the synthesized ligands was focused on in vitro radioligand binding assay and functional assays and in vivo behavioral tests. Basically, the radioligand binding assay was adopted to characterize the affinity and selectivity of new ligands for the MOR, DOR, and KOR, whereas the ^{35}S-GTP[γS]-binding functional assay was applied to determine whether each new ligand acted as an agonist, partial agonist, or antagonist of the MOR by determining its efficacy for G-protein activation relative to a full agonist at the MOR. Agonist efficacy were measured at the level of G-protein activation because efficacy is most accurately determined at this proximal level of signal transduction.[51−53] The use of cell lines heterologously expressing each of the cloned receptors has become standard practice because it provides a pure source of each opioid receptor type free of other opioid receptor types. Furthermore, these systems express the receptor at high density to provide optimal signal-to-noise ratios in the radioligand and ^{35}S-GTP[γS] binding assays. The in vivo tests were focused on the inhibition of morphine's antinociception activity and behavioral properties of those compounds showing high selectivity and low agonist efficacy at the MOR.

In Vitro Pharmacological Study. The primary testing of these ligands included the competitive radioligand binding assay using the monocloned opioid receptors expressed in CHO cell lines. [^{3}H]naloxone, [^{3}H]NTI, and [^{3}H]norBNI were used to label the MOR, DOR, and KOR, respectively. The binding affinities of these ligands to the μ, δ, and κ opioid receptors are summarized in Table 2. Most of these ligands showed subnanomolar affinity for the MOR and significant selectivity for the MOR over DOR and KOR. These results demonstrated that our primary molecular design was successful.

As shown in Table 2, target compounds **1**−**6** all have subnanomolar or nanomolar affinity for the MOR while much lower affinity for the DOR and KOR. Specifically, compound **4** showed over 1000-fold selectivity for the MOR over DOR, whereas compound **6** showed over 700-fold selectivity for the MOR over DOR and over 150-fold selectivity for the MOR over KOR. The control compounds **7** and **8** showed somewhat lower affinity for MOR and lower selectivity for MOR over KOR. These results suggest the possibility of hydrogen bonding or other polar interactions between the target compounds and the MOR because the only unique chemical structure in the target compounds is the nitrogen atom in the pyridine ring.

Similarly, target compounds **9**−**14** all showed high subnanomolar affinity for MOR, whereas compound **9** and **11** exhibited the highest selectivity for the MOR over both the DOR and KOR. Again we observed significantly lower affinity and selectivity of the control compounds **15** and **16** for the MOR. This finding further supported the possibility of hydrogen bonding or some other polar interaction between the target compounds and the MOR because of the existence of a quinoline or isoquinoline ring in the target compounds versus the pure aromatic ring system of the naphthalene moiety in the control compounds.

All of these ligands except the controls (which showed lower affinity for the MOR) were then tested in the 35S-GTP[γS] binding functional assay using the MOR-expressing CHO cell line (Table 3). The ^{35}S-GTP[γS] binding results were analyzed in such a way as to normalize the stimulation produced by each novel ligand to that obtained with the full agonist DAMGO, which provided a measurement of relative efficacy. These results demonstrated that all of the novel ligands showed partial agonism.

Table 1. Ligands Designed as the μ Opioid Receptor Selective Antagonists

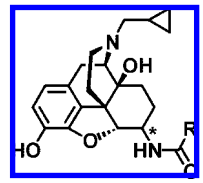

Compound	R	C6-configuration	Compound	R	C6-configuration
1		α	9	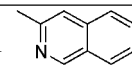	α
2		β	10		β
3		α	11	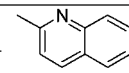	α
4		β	12		β
5	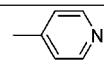	α	13	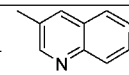	α
6		β	14		β
7	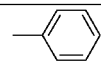	α	15	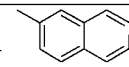	α
8		β	16		β

Scheme 1. Synthetic Route for the Target Compounds Designed

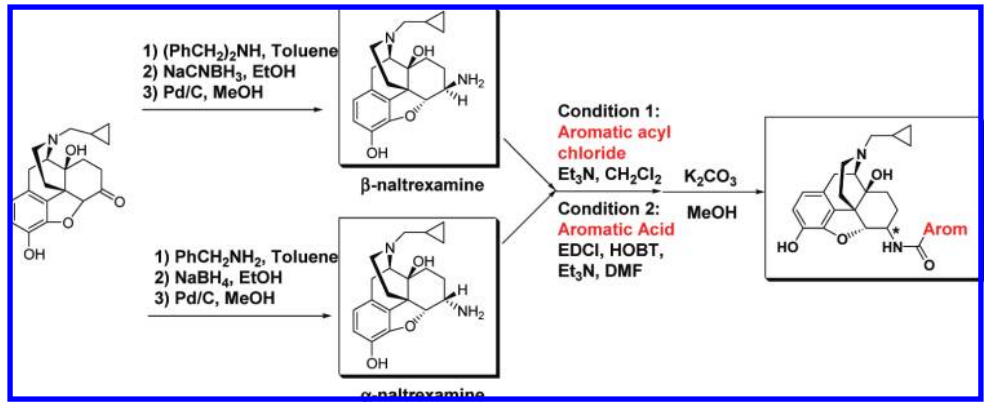

Specifically, compounds **6** and **9** showed the lowest relative efficacy, with approximately 20% of the maximal stimulation produced by DAMGO. Compounds **6** and **9** produced stimulation similar to nalbuphine, a ligand with very low efficacy to activate the MOR. As the main goal of this project is to develop a neutral antagonist of the MOR, their high affinity and selectivity for the MOR and very low agonism at the MOR shed light on our future molecular design. To further characterize their pharmacological profile, we conducted in vivo study of these compounds.

In Vivo Pharmacological Evaluation. The potential MOR selective antagonists were evaluated for acute agonistic and antagonistic effects in mice. In detail, they were tested for their ability to produce antinociception and to antagonize the antinociceptive effects of morphine in the mouse tail immersion test. The data are summarized in Table 4. As shown, both lead compounds, **6** and **9**, were found to be potent antagonists of morphine. Their antagonist AD_{50} values were 4.51 and 0.45 nM, and neither of these ligands produced any agonist effect in this test at doses up to 100 mg/kg. This is in agreement with our original molecular design hypothesis as well as the in vitro functional assays. Therefore, these two compounds may be applied as leads for our next generation of molecular design and synthesis to identify pure, potent, and highly selective antagonists for the MOR. In addition, compounds **1** and **2** had similar ED_{50} values to compound **9** and compounds **4**, **5**, and **13** were equally potent to compound **6** as a morphine antagonist. On the other hand, compound **12** was more potent than morphine, and compounds **10** and **11** were equally potent to morphine in producing antinociception in this test.

Interestingly, some of the target compounds did not show parallel functional activity between the in vitro and the in vivo studies. For example, both lead compounds **6** and **9** showed partial agonism in the ^{35}S-GTP[γS] binding assay while acting as full antagonists in the warm-water tail immersion test. On the other hand, compounds **10**, **11**, and **12** showed only moderately higher partial agonism in the ^{35}S-GTP[γS] binding assay but acted as full agonists in the in vivo assays. To our understanding, there are several factors that might have contributed to these observations. First, it has been reported that the level of antinociception produced by an opioid is dependent on both the intrinsic efficacy of the drug and the stimulus intensity. Some low efficacy MOR partial agonists, such as butorphanol, produced maximal levels of antinociception at a lower temperature nociceptive stimulus (50 °C) but not at a higher temperature (56 °C) stimulus.[54] On the other hand,

Table 2. The Binding Affinity and Selectivity of C(6) Naltrexamine Derivatives ($n = 3$)[a]

	K_i (nM) ± SEM			selectivity ratio	
compd	MOR	DOR	KOR	δ/μ	κ/μ
NTX	0.26 ± 0.02	117.06 ± 8.94	5.15 ± 0.26	450	20
β-FNA	0.41 ± 0.04	27.78 ± 4.60	0.94 ± 0.05	68	2
CTAP	2.02 ± 0.71	1441.0 ± 106.1	1012.7 ± 174.8	713	501
1	2.65 ± 0.42	64.46 ± 15.97	222.58 ± 11.97	24	84
2	5.85 ± 1.41	215.18 ± 21.02	277.96 ± 67.77	37	47
3	0.15 ± 0.07	40.78 ± 8.39	77.23 ± 22.43	265	501
4	0.14 ± 0.04	191.98 ± 15.58	5.42 ± 1.18	1413	40
5	0.48 ± 0.12	186.64 ± 32.07	19.56 ± 9.06	389	41
6 (NAP)	0.37 ± 0.07	277.51 ± 7.97	60.72 ± 5.58	747	163
7	1.41 ± 0.62	385.84 ± 83.99	41.69 ± 6.06	274	30
8	0.92 ± 0.30	478.82 ± 19.94	7.79 ± 1.53	522	8
9 (NAQ)	0.55 ± 0.15	132.50 ± 27.01	26.45 ± 5.22	241	48
10	0.10 ± 0.06	15.42 ± 9.74	1.58 ± 0.68	156	16
11	0.21 ± 0.11	148.20 ± 64.80	9.84 ± 0.96	693	46
12	0.11 ± 0.03	3.86 ± 1.21	5.04 ± 1.30	36	47
13	0.12 ± 0.03	32.19 ± 1.01	1.81 ± 0.11	277	16
14	0.07 ± 0.02	11.61 ± 2.99	0.57 ± 0.20	157	8
15	8.36 ± 1.71	518.32 ± 14.06	608.76 ± 15.77	62	73
16	55.6 ± 3.6	29.26 ± 4.74	65.26 ± 17.26	0.5	1

[a] The K_i values for the μ, δ, and κ opioid receptors are $n = 3$. The averages are reported along with their standard error of the means, SEM, for each compound. The comparison to percent stimulation of DAMGO is the E_{max} of the compound compared to the E_{max} of DAMGO (normalized to 100%). Naltrexone, β-FNA, and CTAP were tested along as positive controls under the same conditions.

Table 3. The Efficacy and Potency of Target Compounds in ^{35}S-GTP[γS]-Binding Functional Assay in the MOR Expressing CHO Cells ($n = 3$)

compd	EC_{50} (nM)	E_{max} (% stim)	% max of DAMGO
DAMGO	45.06 ± 6.63	366.5 ± 23.0	100.0 ± 6.2
1	23.90 ± 4.66	133.5 ± 9.8	37.79 ± 2.68
2	26.28 ± 8.05	150.6 ± 15.8	41.09 ± 4.32
3	1.01 ± 0.40	164.3 ± 16.5	44.82 ± 4.50
4	0.33 ± 0.14	106.7 ± 18.3	29.11 ± 5.00
5	1.26 ± 0.67	136.8 ± 17.8	37.32 ± 4.87
6 (NAP)	1.14 ± 0.38	83.3 ± 3.1	22.72 ± 0.84
9 (NAQ)	4.36 ± 0.72	58.00 ± 9.30	15.83 ± 2.53
10	0.27 ± 0.06	120.9 ± 9.0	32.99 ± 2.46
11	0.09 ± 0.04	239.6 ± 22.5	65.38 ± 6.13
12	0.69 ± 0.19	149.8 ± 26.1	40.87 ± 7.20
13	2.29 ± 0.72	164.3 ± 14.5	44.83 ± 3.96
14	0.29 ± 0.02	195.8 ± 32.0	53.41 ± 8.74

Table 4. AD_{50} Values for Naloxone and the Two Series of C6-Naltrexamine Derivatives vs Morphine in the Warm-Water Tail Immersion Test in Vivo

compd	AD_{50} value (mg/kg (95% CL)) for blockade of morphine antinociception
naloxone	**0.05 (0.03−0.09)**
1	0.89 (0.75−1.07)
2	0.33 (0.26−0.43)
3	36.77 (29.99−44.98)
4	1.38 (0.78−2.43)
5	8.65 (5.35−13.97)
6 (NAP)	4.51 (2.45−8.26)
9 (NAQ)	0.45 (0.27−0.78)
10[a]	inactive
11[b]	inactive
12[c]	inactive
13	4.45 (2.41−8.15)
14	42.55 (23.67−76.51)

[a] Agonist, ED_{50} 1.19 mg/kg (morphine ED_{50} 2.59 mg/kg). [b] Agonist, ED_{50} 4.57 mg/kg. [c] Agonist, ED_{50} 0.04 mg/kg.

butorphanol acted as an antagonist and shifted the dose−effect curve of the high-efficacy opioid alfentanil to the right in a competitive manner at a higher temperature (55 °C) stimulus.[55] This may explain why the two lead compounds did not show any efficacy at the higher temperature (56 °C) stimulus and thereby acted as full antagonists in the in vivo study. Second, some ligands could have significant intrinsic efficacy at the DOR or KOR while acting as low efficacy partial agonists at the MOR, which might explain why compounds **10**, **11**, and **12** acted as full agonists in vivo. The intrinsic efficacy of these novel ligands at the DOR and KOR are currently under study to address this hypothesis.

Further Molecular Modeling Study. To verify that the two lead compounds that acted as selective MOR ligands utilized the alternate "address" domain identified from the previous modeling study, further molecular modeling study was conducted. First, compound **6** and **9** were built using the InsightII/Discover program and their conformation energy minimization was conducted. Then, as we have described for the docking study of naltrexone in the three opioid receptor homology models, they were docked into the homology model of MOR interactively. The orientation of the newly introduced C(6) side chain was not deliberately considered originally. The lowest energy conformation after the minimization and the dynamics simulation of the ligand/receptor complex is illustrated in Figure 5.

As shown in Figure 5A, the C(6) side chain in lead compound **6** pointed to the aromatic binding locus at the extracellular loop region of the MOR. The pyridinyl moiety was in the vicinity of Tyr210 (Yxl2.43) while the distance between the nitrogen atom in the pyridine ring and the oxygen atom in the hydroxyl group of Tyr210 (Yxl2.43) was 3.37 Å. Similarly, the C(6) side chain in lead compound **9** also pointed to the aromatic binding locus at the extracellular loop region of the MOR while the isoquinolinyl moiety in **9** was in the vicinity of Trp318 (W7.35) (Figure 5B). The distance between the nitrogen atom in the isoquinoline ring and the nitrogen atom in the indole ring of Trp318 (W7.35) was 3.64 Å. Both distances could be plausible for hydrogen bonding interaction between the C(6) side chains in the ligands and the specified amino acid residue.

Because these two residues (Tyr210 (Yxl2.43) and Trp318 (W7.35)) are not conserved in the DOR and KOR, it seems that these two residues could act as an alternate "address" domain in MOR, and this plausible hydrogen bonding could contribute to the selectivity of lead compounds **6** and **9** for the MOR. As our molecular models are based on homology modeling of these opioid receptors and are preliminary, site-directed mutagenesis, and radioligand binding analysis with the

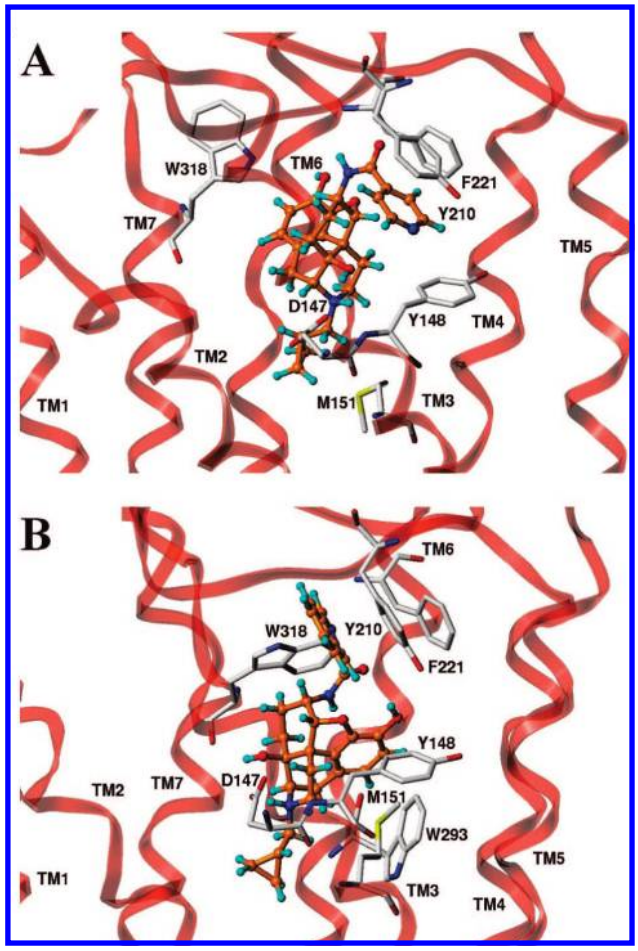

Figure 5. The docking of lead compound **6** and **9** in the μ opioid receptor model. The ligands are in ball and stick, and colored as carbon, red-orange; hydrogen, cyan; oxygen, red and nitrogen, blue; the amino acid residues are in stick and colored as carbon, grey; oxygen, red and nitrogen, blue. The receptor homology model is in red.

mutated MOR will be conducted in future studies to confirm this hypothesis.[56]

Conclusions

In summary, on the basis of the molecular modeling study of the opioid receptor antagonist binding pocket using naltrexone as a probe molecule, an alternative "address" binding domain has been identified in the MOR antagonist binding pocket. Two series of novel ligands have been designed and synthesized to target on this "address" domain as proof-of-concept. Competition binding and in vitro functional assays have identified two lead compounds with subnanomolar affinity for the MOR and high selectivity over the DOR and KOR. Both lead compounds showed partial agonism in the in vitro G-protein activation test and potent antagonism in the in vivo antinociceptive test. Further molecular modeling study has implicated that the selectivity of these two ligands for the MOR could be the result of potential hydrogen bonding between the ligand and the "address" binding locus in the MOR. All of these results will inform our future ligand design in the pursuit of highly selective and pure antagonists of the MOR. Moreover, we have also observed that some of the compounds in these series showed a range of efficacies as MOR partial agonists. These ligands would serve as pharmacological tools to obtain information on MOR activation mechanisms and on structural parameters that affect ligand efficacy at the MOR.

Experimental Section

Molecular Modeling. A Silicon Graphics Octane 2 workstation, equipped with two parallel R12000 processors, was used for all computational studies. InsightII (Accelrys)[57] package was used for modeling. InsightII/Homology module was used to construct the homology models of three opioid receptors based on the X-ray crystal structure of bovine rhodopsin, as reported previously.[39] InsightII/Discover module was applied to construct all the small molecules in their nitrogen-protonated form. Minimization with the steepest descent and then the conjugate gradient algorithm were performed to generate the lowest energy conformation for each ligand studied. Then a molecular dynamics simulation was performed (an equilibration phase of 1000 fs at 300 K, followed by a collection phase of 5000 fs at the same temperature) to further study the small molecule conformation. The lowest energy conformation of the molecule from the last 2 ps molecular dynamics simulation was extracted and applied as the initial configuration for docking into the proposed binding site of the opioid receptors. The docking of the small molecule was conducted interactively using InsightII/Discover. Experimental studies[47] suggest that the protonated nitrogen moiety interacts with the carboxyl group of Asp 147 to form a putative salt bridge. In detail, the molecule was docked in the upper level of transmembrane part in each receptor. The orientation of the molecule skeleton in the binding locus was mainly decided by: first, the putative ionic interaction between the tertiary amino group in naltrexone and the carboxylic group of aspartate on the transmembrane helix 3 in each opioid receptor (Asp147 in μ, Asp128 in δ, and Asp138 in κ); second, the hydrophobic portion of the ligand intend to face the hydrophobic transmembrane helices while the hydrophilic portion to the more polar extracellular loop region. The ligand−receptor complex was minimized in gas phase first with the backbone of the receptor fixed, but all the side chain atoms were left unconstrained. The optimized conformation was then used as the initial configuration for the molecular dynamics simulations. A short-term steepest descent energy minimization (5000 iterations) and dynamics simulation (10000 step, 1 fs each step) was conducted to validate the docking primarily followed by a more vigorous minimizations (50000 iterations) and dynamics simulation (100000 steps) was conducted with 2000 steps equilibration for the initial dynamics. The total simulation time was 102 ps. In both processes, the backbone of the receptor was fixed to prevent the disruption of the α-helical bundle of the receptor and a generic distance constraint (4−4.2 Å) was applied between the negatively charged oxygen atom in aspartate on TM3 and the positively charged nitrogen atom in the ligand. After the dynamics simulation, the lowest energy conformation of the complex was extracted and saved for analysis.

Chemical Synthesis. General Methods. All reagents were purchased from Sigma-Aldrich or as otherwise states. Melting points were obtained with a Fisher Scientific micro melting point apparatus and were uncorrected. All IR spectra were recorded on a Nicolet Avatar 360 FT-IR instrument. Proton (300 MHz) and Carbon-13 (75 MHz) nuclear magnetic resonance (NMR) spectra were recorded at ambient temperature with tetramethylsilane as the internal standard on either a Varian Gemini-300 MHz "Tesla" spectrometer or Varian Mercury-300 MHz NMR spectrometer. GC/MS analysis was performed on a Hewlett-Packard 6890 (Palo Alto, CA). TLC analyses were carried out on the Analtech Uniplate F254 plates. Chromatographic purification was carried out on silica gel columns (230−400 mesh, Merck). Yields were not maximized. The final target compounds' purity was tested by HPLC and elemental analysis, and a satisfying purity of >95% was achieved from both methods. Varian ProStar HPLC System was used on Microsorb-MV 100−5 C18 column (250 mm × 4.6 mm) with injection volume at 10 μL and sample concentrations at 1−2 mg/0.5 mL in 100% acetonitrile; the sample was detected at single wavelength of 210 nm with eluent system of acetonitrile:water (75:25) at 1 mL/min over 50 min. Elemental analysis was conducted in Atlantic

Microlab, Inc. All spectral data reported here were obtained from the hydrochloride salt form of the products while compounds **1**−**6** and **9**−**14** were dihydrochloride salts, and compounds **7**, **8**, **15**, and **16** monohydrochloride salts.

General Procedure 1. A solution of 6α-naltrexamine or 6β-naltrexamine (1 equiv) in CH_2Cl_2 was added acyl chloride (2 equiv) and triethylamine (4 equiv) on an ice−water bath under N_2 protection. The mixture was allowed to stir overnight at room temperature. After concentrated to remove CH_2Cl_2, the resulting residue was dissolved in MeOH and potassium carbonate (2 equiv) added. The reaction mixture was stirred overnight at room temperature. After concentration, the residue was partitioned between water and CH_2Cl_2. The water layer was extracted with CH_2Cl_2. The combined CH_2Cl_2 solution was washed with brine and dried over Na_2SO_4. After concentration, the residue was purified by silica gel column with a CH_2Cl_2/MeOH (100:1) (1% NH_3H_2O) solvent system as eluent to give the aim product. The product was then transferred into the hydrochloride salt using 1.25 M hydrochloride acid methanol solution at 0 °C.

General Procedure 2. A solution of carboxylic acid (3 equiv) in DMF was added *N*-(3-dimethylaminopropyl)-*N*′-ethylcarbodiimide hydrochloride (EDCI, 2.5 equiv), hydrobenzotriazole (HOBt, 2.5 equiv), 4 Å molecular sieve, and triethylamine (5 equiv) on an ice−water bath under N_2 protection. After 15 min, a solution of 6β-naltrexamine (1 equiv) in DMF was added. The reaction mixture was filtered over celite after stirring overnight at room temperature. The filtrate was concentrated in vacuum to remove DMF. The residue was dissolved in MeOH and added potassium carbonate (2 equiv). The resulting mixture was stirred overnight at room temperature. After concentration, the residue was partitioned between water and CH_2Cl_2. The water layer was extracted with CH_2Cl_2. The combined CH_2Cl_2 solution was washed with H_2O, brine, and dried with Na_2SO_4. After concentration, the residue was purified by silica gel column with a CH_2Cl_2/MeOH (100:1) (1% NH_3H_2O) solvent system as eluent to give the aim product. Then the product was transferred into a hydrochloride salt.

17-Cyclopropylmethyl-3,14β-dihydroxy-4,5α-epoxy-6α-[(2′-pyridyl)acetamido]morphinan (1). Compound **1** was prepared by following the general procedure 1 in 58% yield; $[\alpha]^{25}_D$ −244° (*c* = 0.05, MeOH); mp 212−214 °C. IR (KBr, cm^{-1}) ν_{max}: 3225, 1675, 1521, 1320. ^{1}H NMR (300 MHz, DMSO): δ 8.90 (b, 1 H, exchangeable), 8.71 (b, 1 H, amide-H), 8.39 (m, 1 H, Ar−H), 8.09 (m, 2 H, Ar−H), 7.68 (m, 1 H, Ar−H), 6.77 and 6.62 (2 d, 1 H each, *J* = 8.1 Hz, C_1−H, C_2−H), 4.77 (m, 1 H, C_6−H), 4.67 (m, 1 H, C_5−H), 3.12 (d, *J* = 6.3 Hz, 1 H), 3.05 (d, *J* = 18.6 Hz, 1 H), 2.67 (m, 1 H), 2.63 (m, 1 H), 2.57 (m, 1 H), 2.35 (m, 1 H), 2.27 (m, 1 H), 2.17 (m, 2 H), 1.84 (m, 1 H), 1.74 (m, 1 H), 1.49 (m, 1 H), 1.14 (m, 1 H), 0.86 (m, 1 H), 0.54 (m, 2 H), 0.12 (m, 2 H). ^{13}C NMR (75 MHz, DMSO) δ: 163.88, 150.16, 148.34, 145.74, 137.79, 137.61, 130.10, 126.35, 125.99, 122.69, 119.41, 117.61, 90.45, 69.85, 62.36, 59.91, 47.49, 46.49, 43.39, 33.83, 29.45, 23.11, 21.17, 9.60, 4.21, 4.06. MS (ESI) *m*/*z*: 447.7 (M^+). Anal. ($C_{26}H_{29}N_3O_4$·2HCl·1.5H_2O) C, H.

17-Cyclopropylmethyl-3,14β-dihydroxy-4,5α-epoxy-6β-[(2′-pyridyl)acetamido]morphinan (2). Compound **2** was prepared by following the general procedure 1 in 65% yield; $[\alpha]^{25}_D$ −91° (*c* = 0.07, MeOH); mp 210−212 °C. IR (KBr, cm^{-1}) ν_{max}: 3384 1673, 1526, 1324. ^{1}H NMR (300 MHz, DMSO): δ 9.07 (b, 1 H, amide-H), 8.86 (b, 1 H, exchangeable), 8.69 (m, 1 H, Ar−H), 8.03 (m, 2 H, Ar−H), 7.65 (m, 1 H, Ar−H), 6.73 and 6.68 (2 d, 1 H each, *J* = 8.1 Hz, C_1−H, C_2−H), 5.02 (m, 1 H, C_6−H), 4.62 (m, 1 H, C_5−H), 3.10 (d, *J* = 6.3 Hz, 1 H), 3.03 (d, *J* = 18.9 Hz, 1 H), 2.65 (m, 1 H), 2.63 (m, 1 H), 2.58 (m, 1 H), 2.37 (m, 2 H), 2.25 (m, 1 H), 2.19 (m, 1 H), 1.95 (m, 1 H), 1.82 (m, 1 H), 1.61 (m, 1 H), 1.45 (m, 1 H), 0.84 (m, 1 H), 0.54 (m, 2 H), 0.12 (m, 2 H). ^{13}C NMR (75 MHz, DMSO) δ: 160.27, 145.86, 144.30, 138.97, 136.63, 133.54, 127.19, 122.39, 120.28, 118.59, 115.29, 114.35, 89.11, 66.42, 58.54, 55.44, 47.84, 43.91, 41.96, 40.30, 27.00, 26.22, 20.59, 18.88, 6.82, 5.68. MS (ESI) *m*/*z*: 448.1 (M + H)$^+$. Anal. ($C_{26}H_{29}N_3O_4$·2HCl·3H_2O) C, H.

17-Cyclopropylmethyl-3,14β-dihydroxy-4,5α-epoxy-6α-[(3′-pyridyl)acetamido]morphinan (3). Compound **3** was prepared by following the general procedure 1 in 54% yield; $[\alpha]^{25}_D$ −273° (*c* = 0.06, MeOH); mp 211−214 °C. IR (KBr, cm^{-1}) ν_{max}: 3215, 1672, 1531, 1507, 1322. ^{1}H NMR (300 MHz, DMSO): δ 9.23 (m, 1 H, Ar−H), 8.94 (b, 1 H, exchangeable), 8.92 (s, 1 H, amide-H), 8.75 (d, *J* = 5.1.Hz, 1 H, Ar−H), 8.66 (d, *J* = 7.5 Hz, 1 H, Ar−H), 7.89 (dd, *J* = 5.1, 7.5 Hz, 1 H, Ar−H), 6.73 and 6.58 (2 d, 1 H each, *J* = 8.1 Hz, C_1−H, C_2−H), 4.76 (m, 1 H, C_5−H), 4.63 (m, 1 H, C_6−H), 3.97 (m, 1 H), 3.43 (m, 2 H), 3.05 (m, 3 H), 2.71 (m, 1 H), 2.45 (m, 2 H), 1.95 (m, 1 H), 1.63 (m, 1 H), 1.53 (m, 1 H), 1.20 (m, 1 H), 1.06 (m, 1 H), 0.64 (m, 2 H), 0.45 (m, 2 H). ^{13}C NMR (75 MHz, DMSO) δ: 165.25, 151.34, 147.83, 145.94, 138.43, 136.20, 131.16, 130.84, 125.51, 123.82, 119.56, 117.96, 89.49, 69.88, 62.38, 59.89, 47.28, 45.95, 43.45, 33.71, 29.32, 23.08, 21.38, 9.62, 4.20, 4.06. MS (ESI) *m*/*z*: 448.9 (M + H)$^+$. Anal. ($C_{26}H_{29}N_3O_4$·2HCl·3H_2O) C, H.

17-Cyclopropylmethyl-3,14β-dihydroxy-4,5α-epoxy-6β-[(3′-pyridyl)acetamido]morphinan (4). Compound **4** was prepared by following the general procedure 1 in 56% yield; $[\alpha]^{25}_D$ −141° (*c* = 0.10, MeOH). mp 225−227 °C. IR (KBr, cm^{-1}) ν_{max}: 3207, 3057, 1665, 1540, 1326. ^{1}H NMR (300 MHz, DMSO): δ 9.18 (m, 1 H, Ar−H), 9.15 (b, 1 H, amide-H), 8.90 (b, 1 H, exchangeable), 8.86 (m, 1 H, Ar−H), 8.51 (m, 1 H, Ar−H), 7.77 (m, 1 H, Ar−H), 6.75 and 6.68 (2 d, 1 H each, *J* = 8.4 Hz, C_1−H, C_2−H), 4.85 (d, *J* = 8.4 Hz, 1 H, C_5−H), 4.47 (s, 1 H, C_6−H), 3.89 (m, 1 H), 3.73 (m, 1 H), 3.38 (m, 1 H), 3.12 (m, 2 H), 2.85 (m, 1 H), 2.45 (m, 2 H), 1.93 (m, 1 H), 1.80 (m, 1 H), 1.64 (m, 1 H), 1.47 (m, 2 H), 1.09 (m, 1 H), 0.64 (m, 2 H), 0.46 (m, 2 H). ^{13}C NMR (75 MHz, DMSO) δ: 161.34, 147.63, 144.05, 139.39, 136.30, 131.90, 126.87, 126.46, 120.29, 119.68, 115.32, 114.28, 88.05, 66.55, 58.39, 55.48, 47.27, 41.88, 40.16, 27.77, 25.51, 19.75, 18.82, 6.98, 5.63, 3.26. MS (ESI) *m*/*z*: 448.9 (M + H)$^+$. Anal. ($C_{26}H_{29}N_3O_4$·2HCl·3H_2O) C, H.

17-Cyclopropylmethyl-3,14β-dihydroxy-4,5α-epoxy-6α-[(4′-pyridyl)acetamido]morphinan (5). Compound **5** was prepared by following the general procedure 1 in 45% yield; $[\alpha]^{25}_D$ −213° (*c* = 0.09, MeOH); mp 215−217 °C. IR (KBr, cm^{-1}) ν_{max}: 3225, 1653, 1542, 1500, 1318. ^{1}H NMR (300 MHz, DMSO): δ 8.92 (m, 2 H, Ar−H), 8.88 (b, 1 H, exchangeable), 8.77 (b, 1 H, amide-H), 8.08 (m, 2 H, Ar−H), 6.73 and 6.59 (2 d, 1 H each, *J* = 8.1 Hz, C_1−H, C_2−H), 4.78 (m, 1 H, C_5−H), 4.62 (m, 1 H, C_6−H), 3.95 (m, 1 H), 3.40 (m, 2 H), 3.06 (m, 2 H), 2.74 (m, 1 H), 2.46 (m, 2 H), 1.91 (m, 1 H), 1.65 (m, 1 H), 1.52 (m, 1 H), 1.18 (m, 2 H), 1.09 (m, 1 H), 0.69 (m, 2 H), 0.49 (m, 2 H). ^{13}C NMR (75 MHz, DMSO) δ: 164.17, 149.72, 149.72, 145.15, 142.08, 137.77, 130.25, 124.71, 121.12, 121.12, 119.07, 117.28, 88.82, 69.06, 61.74, 59.26, 46.81, 46.54, 45.27, 42.58, 33.29, 28.70, 22.43, 8.17, 7.55, 3.56. MS (ESI) *m*/*z*: 448.9 (M + H)$^+$. Anal. ($C_{26}H_{29}N_3O_4$·2HCl·3H_2O) C, H.

17-Cyclopropylmethyl-3,14β-dihydroxy-4,5α-epoxy-6β-[(4′-pyridyl)acetamido]morphinan (6, NAP). Compound **6** was prepared by following the general procedure 1 in 45% yield; $[\alpha]^{25}_D$ −176° (*c* = 0.01, MeOH); mp 258−61 °C. IR (KBr, cm^{-1}) ν_{max}: 3386, 1666, 1548, 1502, 1326. ^{1}H NMR (300 MHz, DMSO): δ 8.81 (b, 1 H, amide-H), 8.45 (m, 2 H, Ar−H), 8.22 (b, 1 H, exchangeable), 7.60 (m, 2 H, Ar−H), 6.32 and 6.27 (2 d, 1 H each, *J* = 7.8 Hz, C_1−H, C_2−H), 4.84 (s, 1 H, C_5−H), 4.46 (m, 1 H, C_6−H), 3.90 (m, 1 H), 3.69 (m, 1 H), 3.30 (m, 2 H), 3.06 (m, 2 H), 2.85 (m, 1 H), 2.45 (m, 2 H), 1.93 (m, 1 H), 1.80 (m, 1 H), 1.59 (m, 1 H), 1.46 (m, 1 H), 1.07 (m, 1 H), 0.63 (m, 2 H), 0.45 (m, 2 H). ^{13}C NMR (75 MHz, DMSO) δ: 164.30, 149.27, 142.72, 139.62, 130.15, 128.61, 127.80, 124.87, 123.73, 120.89, 118.86, 117.84, 91.15, 69.90, 61.75, 58.84, 50.68, 46.91, 43.50, 39.98, 31.10, 28.60, 22.18, 8.99, 3.68, 3.37. MS (ESI) *m*/*z*: 448.9 (M + H)$^+$. Anal. ($C_{26}H_{29}N_3O_4$·2HCl·3H_2O) C, H.

17-Cyclopropylmethyl-3,14β-dihydroxy-4,5α-epoxy-6α-(benzamido)morphinan (7). Compound **7** was prepared by following the general procedure 1 in 54% yield; $[\alpha]^{25}_D$ −215° (*c* = 0.11, MeOH); mp 182−185 °C. IR (KBr, cm^{-1}) ν_{max}: 3353, 2947, 1638, 1540, 1324. ^{1}H NMR (300 MHz, DMSO): δ 7.75 (m, 2 H, Ar−H), 7.45 (m, 3 H, Ar−H), 6.70 and 6.65 (2 d, 1 H each, *J* = 8.4 Hz, C_1−H, C_2−H), 6.50 (b, 1 H, amide-H), 4.79 (m, 1 H, C_6−H), 4.77

(m, 1 H, C_5−H), 3.14 (m, 1 H), 3.04 (m, 1 H), 2.68 (m, 1 H), 2.65 (m, 1 H), 2.60 (m, 1 H), 2.36 (m, 1 H), 2.29 (m, 1 H), 2.27 (m, 2 H), 1.84 (m, 1 H), 1.58 (m, 1 H), 1.42 (m, 1 H), 1.25 (m, 1 H), 0.86 (m, 1 H), 0.54 (m, 2 H), 0.12 (m, 2 H). ^{13}C NMR (75 MHz, DMSO) δ: 167.72, 145.85, 138.14, 134.53, 131.57, 131.11, 128.60, 127.47, 125.63, 119.38, 117.86, 90.12, 69.91, 62.32, 59.87, 47.38, 46.98, 43.39, 33.69, 29.45, 23.11, 21.17, 9.56, 4.24, 4.08. MS (ESI) *m/z*: 447.9 $(M + H)^+$. Anal. ($C_{27}H_{30}N_2O_4 \cdot HCl \cdot 2.75H_2O$) C, H.

17-Cyclopropylmethyl-3,14β-dihydroxy-4,5α-epoxy-6β-(benzamido)morphinan (8). Compound **8** was prepared by following the general procedure 1 in 59% yield; $[\alpha]^{25}_D$ −157° (c = 0.07, MeOH); mp 220−221 °C. IR (KBr, cm^{-1}) ν_{max}: 3242, 1638, 1540, 1324. ^{1}H NMR (300 MHz, DMSO): δ 7.84 (m, 2 H, Ar−H), 7.50−7.40 (m, 3 H, Ar−H), 7.21 (b, 1H, amide-H), 6.75 and 6.58 (2 d, 1 H each, J = 8.1 Hz, C_1−H, C_2−H), 4.52 (m, 1 H, C_5−H), 4.26 (m, 1 H, C_6−H), 3.87 (m, 1 H), 3.73 (m, 1 H), 3.15 (m, 1 H), 2.69 (m, 1 H), 2.61 (m, 1 H), 2.40 (m, 1 H), 2.23 (m, 2 H), 1.87 (m, 1 H), 1.72 (m, 1 H), 1.55 (m, 1 H), 1.26 (m, 1 H), 1.12 (m, 1 H), 0.86 (m, 1 H), 0.54 (m, 2 H), 0.12 (m, 2 H). ^{13}C NMR (75 MHz, DMSO) δ: 168.79, 142.59, 140.78, 134.52, 131.55, 131.18, 128.38, 127.23, 123.87, 119.04, 117.62, 91.82, 70.59, 62.61, 58.92, 52.14, 44.49, 30.45, 30.11, 29.66, 24.35, 22.52, 8.76, 3.61, 3.05. MS (ESI) *m/z*: 447.9 $(M + H)^+$. Anal. ($C_{27}H_{30}N_2O_4 \cdot HCl \cdot 3.25H_2O$) C, H.

17-Cyclopropylmethyl-3,14β-dihydroxy-4,5α-epoxy-6α-[(3′-isoquinolyl)acetamido]morphinan (9, NAQ). Compound **9** was prepared by following the general procedure 2 in 70% yield; $[\alpha]^{25}_D$ −150° (c = 0.01, MeOH); mp: 210−213 °C. IR (KBr, cm^{-1}) ν_{max}: 3222, 1666, 1529, 1261, 801. ^{1}H NMR (300 MHz, DMSO): δ 9.44 (s, 1 H, Ar−H), 8.95 (b, 1 H, exchangeable), 8.64 (s, 1 H, Ar−H), 8.58 (b, 1 H, amide-H), 8.27 (m, 2 H, Ar−H), 7.90 (m, 2 H, Ar−H), 6.79 and 6.62 (2 d, 1 H each, J = 7.8 Hz, C_1−H, C_2−H), 4.81 (s, 1 H, C_5−H), 4.74 (m, 1 H, C_6−H), 3.99 (m, 1 H), 3.45 (m, 2 H), 3.14 (m, 2 H), 2.73 (m, 1 H), 2.58 (m, 1 H), 2.23 (m, 2 H), 1.87 (m, 1 H),1.67 (m, 2 H), 1.48 (m, 1 H), 1.08 (m, 1 H), 0.67 (m, 2 H), 0.47 (m, 2 H). ^{13}C NMR (75 MHz, DMSO) δ: 159.97, 148.87, 146.15, 139.18, 138.21, 137.40, 134.48, 132.47, 131.01, 128.93, 128.86, 128.37, 124.16, 122.44, 120.07, 118.39, 87.91, 69.86, 62.26, 57.93, 47.15, 46.05, 30.51, 29.43, 23.88, 19.57, 19.56, 5.75, 5.18, 2.26. MS (ESI) *m/z*: 498.1 $(M + H)^+$. Anal. ($C_{30}H_{31}N_3O_4 \cdot 2HCl \cdot 0.5H_2O$) C, H.

17-Cyclopropylmethyl-3,14β-dihydroxy-4,5α-epoxy-6β-[(3′-isoquinolyl)acetamido]morphinan (10). Compound **10** was prepared by following the general procedure 2 in 50% yield; $[\alpha]^{25}_D$ −166° (c = 0.10, MeOH); mp 235−237 °C. IR (KBr, cm^{-1}) ν_{max}: 3069, 1665, 1537, 1328, 901. ^{1}H NMR (300 MHz, DMSO): δ 9.46 (s, 1H, Ar−H), 9.27 (b, 1 H, amide-H), 9.15 (s, 1 H, Ar−H), 8.92 (b, 1 H, exchangeable), 8.21 (m, 2 H, Ar−H), 8.00 (m, 1 H, Ar−H), 7.81 (m, 1 H, Ar−H), 6.76 and 6.68 (2 d, 1 H each, J = 8.4 Hz, C_1−H, C_2−H), 5.06 (m, 1 H, C_6−H), 4.90 (d, J = 7.8 Hz, 1 H, C_5−H), 3.91 (m, 1 H), 3.78 (m, 1 H), 3.37 (m, 2 H), 3.10 (m, 2 H), 2.89 (m, 1 H), 2.45 (m, 1 H), 2.00 (m, 1 H), 1.83 (m, 1 H), 1.69 (m, 1 H), 1.49 (m, 2 H), 1.12 (m, 1 H), 0.68 (m, 2 H), 0.48 (m, 2 H). ^{13}C NMR (75 MHz, DMSO) δ: 164.63, 151.51, 143.09, 142.94, 140.57, 135.84, 131.37, 131.26, 129.64, 129.01, 128.16, 128.06, 124.62, 120.53, 119.48, 118.30, 92.95, 62.55, 59.43, 52.26, 44.35, 36.71, 31.66, 30.85, 30.42, 24.69, 22.92, 9.68, 4.22, 4.02. MS (ESI) *m/z*: 498.8 $(M + H)^+$. Anal. ($C_{30}H_{31}N_3O_4 \cdot 2HCl \cdot 3.5H_2O$) C, H.

17-Cyclopropylmethyl-3,14β-dihydroxy-4,5α-epoxy-6α-[(2′-quinolyl)acetamido]morphinan (11). Compound **11** was prepared by following the general procedure 1 in 93% yield. The product was transferred into a HCl salt; $[\alpha]^{25}_D$ −186° (c = 0.03, MeOH); mp 212−214 °C. IR (KBr, cm^{-1}) ν_{max}: 3199, 1673, 1528, 1321, 785. ^{1}H NMR (300 MHz, DMSO): δ 8.90 (b, 1 H, amide-H), 8.60 (m, 2 H, Ar−H), 8.21 (b, 1 H, exchangeable), 8.13 (m, 2H, Ar−H), 7.92 (m, 1 H, Ar−H), 7.75 (m, 1 H, Ar−H), 6.76 and 6.63 (2 d, 1 H each, J = 7.8 Hz, C_1−H, C_2−H), 4.84 (s, 1 H, C_5−H), 4.68 (m, 1 H, C_6−H), 3.94 (m, 1 H), 3.65 (m, 1 H), 3.35 (m, 1 H), 3.05 (m, 1 H), 2.71 (m, 1 H), 2.45 (m, 2 H), 1.93 (m, 2 H), 1.82 (m, 1 H), 1.65 (m, 1 H), 1.48 (m, 2 H), 1.06 (m, 1 H), 0.63 (m, 2 H), 0.44 (m, 2 H). ^{13}C NMR (75 MHz, DMSO) δ: 160.77, 146.72, 146.08, 145.15, 141.05, 139.27, 134.49, 134.49, 130.24, 130.24, 128.88, 123.95, 122.35, 120.10, 119.33, 118.51, 87.79, 69.88, 62.24, 57.95, 47.18, 46.06, 30.51, 29.42, 23.91, 19.68, 19.68, 5.79, 5.22, 2.31. MS (ESI) *m/z*: 498.1 $(M + H)^+$. Anal. ($C_{30}H_{31}N_3O_4 \cdot 2HCl \cdot 2.5H_2O$) C, H.

17-Cyclopropylmethyl-3,14β-dihydroxy-4,5α-epoxy-6β-[(2′-quinolyl)acetamido]morphinan (12). Compound **12** was prepared by following the general procedure 1 in 83% yield; $[\alpha]^{25}_D$ −112° (c = 0.1, MeOH); mp 227−229 °C. IR (KBr, cm^{-1}) ν_{max}: 3110, 1671, 1533, 1329, 770. ^{1}H NMR (300 MHz, DMSO): δ 9.26 (m, 1 H, Ar−H), 8.94 (b, 1 H, amide-H), 8.61 (m, 1 H, Ar−H), 8.16 (m, 2 H, Ar−H), 8.12 (b, 1 H, exchangeable), 7.92 (m, 1 H, Ar−H), 7.78 (m, 1 H, Ar−H), 6.79 and 6.68 (2 d, 1 H each, J = 7.8 Hz, C_1−H, C_2−H), 5.15 (s, 1 H, C_5−H), 5.12 (m, 1 H, C_6−H), 3.93 (m, 1 H), 3.77 (m, 1 H), 3.43 (m, 1 H), 3.10 (m, 2 H), 2.90 (m, 1 H), 2.45 (m, 2 H), 2.09 (m, 1 H), 1.83 (m, 1 H), 1.62 (m, 1 H), 1.48 (m, 1 H), 1.08 (m, 1 H), 0.86 (m, 1 H), 0.65 (m, 2 H), 0.50 (m, 2 H). ^{13}C NMR (75 MHz, DMSO) δ: 163.98, 149.09, 145.84, 141.98, 139.75, 136.87, 130.48, 129.60, 129.12, 128.72, 127.40, 127.26, 123.60, 118.64, 118.44, 117.41, 93.02, 69.83, 61.83, 58.76, 51.23, 47.33, 43.66, 30.11, 29.71, 24.20, 22.20, 8.99,3.62, 3.36. MS (ESI) *m/z*: 497.8 $(M + H)^+$. Anal. ($C_{30}H_{31}N_3O_4 \cdot 2HCl \cdot 0.5H_2O$) C, H.

17-Cyclopropylmethyl-3,14β-dihydroxy-4,5α-epoxy-6α-[(3′-quinolyl)acetamido]morphinan (13). Compound **13** was prepared by following the general procedure 2 in 61% yield; $[\alpha]^{25}_D$ −192° (c = 0.05, MeOH); mp > 270 °C. IR (KBr, cm^{-1}) ν_{max}: 3221, 1660, 1537, 1318, 777. ^{1}H NMR (300 MHz, DMSO): δ 9.39 (s, 1 H, Ar−H), 9.06 (s, 1 H, Ar−H), 8.90 (b, 1 H, amide-H), 8.66 (b, 1 H, exchangeable), 8.19 (m, 2 H, Ar−H), 7.97 (m, 1 H, Ar−H), 7.79 (m, 1 H, Ar−H), 6.73 and 6.59 (2 d, 1 H each, J = 8.1 Hz, C_1−H, C_2−H), 4.83 (m, 1 H, C_5−H), 4.70 (m, 1 H, C_6−H), 3.95 (m, 1 H), 3.45 (m, 2 H), 3.08 (m, 3 H), 2.72 (m, 1 H), 2.52 (m, 2 H), 1.92 (m, 1 H), 1.65 (m, 1 H), 1.51 (m, 1 H), 1.26 (m, 1 H), 1.10 (m, 1 H), 0.68 (m, 2 H), 0.45 (m, 2 H). ^{13}C NMR (75 MHz, DMSO) δ: 164.04, 147.59, 146.84, 144.48, 141.03, 139.52, 134.19, 130.41, 129.48, 128.03, 127.76, 125.83, 122.91, 119.93, 119.24, 116.95, 87.73, 70.15, 61.65, 57.70, 47.08, 45.99, 39.40, 30.92, 29.83, 24.30, 20.10, 6.50, 5.99, 3.34. MS (ESI) *m/z*: 498.9 $(M + H)^+$. Anal. ($C_{30}H_{31}N_3O_4 \cdot 2HCl \cdot 3.75H_2O$) C, H.

17-Cyclopropylmethyl-3,14β-dihydroxy-4,5α-epoxy-6β-[(3′-quinolyl)acetamido]morphinan (14). Compound **14** was prepared by following the general procedure 2 in 87% yield; $[\alpha]^{25}_D$ −86° (c = 0.07, MeOH); Mp 235−238 °C. IR (KBr, cm^{-1}) ν_{max}: 3072, 1660, 1549, 1324, 777. ^{1}H NMR (300 MHz, DMSO): δ 9.47 (s, 1 H, Ar−H), 9.35 (b, 1 H, amide-H), 8.92 (b, 1 H, exchangeable), 8.23 (m, 2 H, Ar−H), 8.22 (s, 1 H, Ar−H), 8.03 (m, 2 H, Ar−H), 6.76 and 6.68 (2 d, 1 H each, J = 8.4 Hz, C_1−H, C_2−H), 5.11 (s, 1 H, C_5−H) 5.01 (m, 1 H, C_6−H), 3.92 (m, 1 H), 3.78 (m, 1 H), 3.33 (m, 2 H), 3.07 (m, 2 H), 2.89 (m, 1 H), 1.83 (m, 1 H), 1.62 (m, 2 H), 1.46 (m, 3 H), 1.11 (m, 1 H), 0.65 (m, 2 H), 0.47 (m, 2 H). ^{13}C NMR (75 MHz, DMSO) δ: 165.68, 147.82, 147.72, 141.71, 140.27, 135.74, 131.00, 130.18, 128.40, 127.21, 127.04, 126.69, 126.50, 122.65, 118.42, 116.87, 99.79, 69.75, 61.90, 57.95, 51.63, 46.22, 44.11, 29.40, 29.24, 23.49, 21.82, 7.55, 2.99, 2.10. MS (ESI) *m/z*: 498.8 $(M + H)^+$. Anal. ($C_{30}H_{31}N_3O_4 \cdot 2HCl \cdot 2.5H_2O$) C, H.

17-Cyclopropylmethyl-3,14β-dihydroxy-4,5α-epoxy-6α-[(2′-naphthalyl)acetamido]morphinan (15). Compound **15** was prepared by following the general procedure 1 in 46% yield; $[\alpha]^{25}_D$ −218° (c = 0.01, MeOH); mp 213−215 °C. IR (KBr, cm^{-1}) ν_{max}: 3399, 1641, 1503, 1460, 1318. ^{1}H NMR (300 MHz, DMSO): δ 8.15 (s, 1 H, Ar−H), 7.77−7.73 (m, 4 H, Ar−H), 7.45 (m, 2 H, Ar−H), 6.85 (b, 1 H, amide-H), 6.85 and 6.50 (2 d, 1 H each, J = 8.1 Hz, C_1−H, C_2−H), 4.80 (m, 1 H, C_6−H), 4.71 (m, 1 H, C_5−H), 3.69 (m, 1 H), 3.00 (m, 1 H), 2.63 (m, 1 H), 2.53 (m, 1 H), 2.34 (m, 1 H), 2.23 (m, 1 H), 2.15 (m, 2 H), 1.76 (m, 1 H), 1.49 (m, 1 H), 1.36 (m, 1 H), 1.09 (m, 1 H), 1.14 (m, 1 H), 0.83 (m, 1 H), 0.55 (m, 2 H), 0.12 (m, 2 H). ^{13}C NMR (75 MHz, CD_3OD) δ: 167.96, 145.46, 138.32, 134.35, 132.03, 130.76, 128.13, 127.44, 127.37, 127.25, 127.17, 127.00, 125.98, 123.30, 121.61, 119.24,

117.59, 87.72, 61.56, 57.25, 44.50, 39.95, 37.39, 29.81, 28.96, 23.29, 18.95, 13.60, 9.87, 5.05, 4.55. MS (ESI) *m/z*: 496.8 (M^+). Anal. ($C_{31}H_{32}N_2O_4 \cdot HCl \cdot 1.5H_2O$) C, H.

17-Cyclopropylmethyl-3,14β-dihydroxy-4,5α-epoxy-6β-[(2′-naphthalyl)acetamido]morphinan (16). Compound **16** was prepared by following the general procedure 1 in 44% yield; $[\alpha]^{25}_D$ −123° (c = 0.09, MeOH); mp 212−215 °C. IR (KBr, cm^{-1}) ν_{max}: 3248, 2964, 1640, 1508, 1319, 716. ^{1}H NMR (300 MHz, DMSO): δ 8.36 (b, 1 H, amide-H), 7.95−7.86 (m, 5 H, Ar−H), 7.56 (m, 2 H, Ar−H), 6.76 and 6.59 (2 d, 1 H each, J = 8.4 Hz, C_1−H, C_2−H), 4.60 (m, 1 H, C_5−H), 4.31 (m, 1 H, C_6−H), 3.88 (m, 1 H), 3.75 (m, 1 H), 3.19 (m, 1 H), 2.70 (m, 1 H), 2.42 (m, 1 H), 2.27 (m, 2 H), 1.96 (m, 1 H), 1.70 (m, 1 H), 1.54 (m, 1 H), 1.24 (m, 1 H), 1.49 (m, 1 H), 1.14 (m, 1 H), 0.88 (m, 1 H), 0.50 (m, 2 H), 0.12 (m, 2 H). ^{13}C NMR (75 MHz, DMSO) δ:. 166.36, 147.21, 142.86, 134.85, 132.86, 131.80, 129.57, 128.98, 128.57, 128.35, 128.25, 128.24, 127.48, 124.85, 121.75, 119.20, 119.10, 91.30, 70.44, 62.43, 51.74, 42.96, 35.67, 33.08, 32.17, 30.45, 24.70, 20.10, 9.50, 6.80, 4.00. MS (ESI) *m/z*: 497.8 $(M + H)^+$. Anal. ($C_{31}H_{32}N_2O_4 \cdot HCl \cdot H_2O$) C, H.

In Vitro Competitive Radioligand-Binding and Functional Assay. Details of the binding assay was conducted to study the selectivity of the ligands by using monocloned opioid receptor expressed in Chinese hamster ovarian (CHO) cell lines as described previously.[44,45] [^{3}H]naloxone, [^{3}H]NTI, and [^{3}H]norBNI were used to label the μ, δ, and κ opioid receptors, respectively. Aliquots of a membrane preparation were incubated with the radioligands in the presence of different concentrations of the drug under investigation at 30 °C for 1 h. Specific (i.e., opioid receptor related) binding was determined as the difference in binding obtained in the absence and presence of 10 μM naltrexone. The potency of the drugs in displacing the specific binding of the radioligand was determined from data using linear regression analysis of Hill plots. The IC_{50} values will then be determined and corrected to K_i values using the Cheng−Prusoff equation. Functional assays, including ^{35}S-GTP[γS]-binding assay, were conducted in the same cell membranes used for the receptor binding assays. Three μM of DAMGO was included in the assay for a maximally effective concentration of a full agonist for the μ opioid receptor.

In Vivo Acute Function Test Procedure. Animals. Male Swiss Webster mice (Harlan Laboratories, Indianapolis, IN) weighing 25−30 g were housed six to a cage in animal care quarters and maintained at 22 ± 2 °C on a 12 h light−dark cycle. Food and water were available ad libitum. The mice were brought to a test room (22 ± 2 °C, 12 h light−dark cycle), marked for identification and allowed 18 h to recover from transport and handling. Protocols and procedures were approved by the Institutional Animal Care and Use Committee (IACUC) at Virginia Commonwealth University Medical Center and comply with the recommendations of the IASP (International Association for the Study of Pain).

Tail Immersion Test. The warm-water tail immersion test was performed according to Coderre and Rollman[58] using a water bath with the temperature maintained at 56 ± 0.1 °C. Before injecting the mice, a baseline (control) latency was determined. Only mice with a control reaction time from 2 to 4 s were used. The average baseline latency for these experiments was 3.0 ± 0.1 s. The test latency after drug treatment was assessed at the appropriate time, and a 10 s maximum cutoff time was imposed to prevent tissue damage. Antinociception was quantified according to the method of Harris and Pierson[59] as the percentage of maximum possible effect (% MPE), which was calculated as: %MPE = [(test latency − control latency)/(10 − control latency)] × 100. Percent MPE was calculated for each mouse using at least six mice per drug.

Drugs. Morphine sulfate was purchased from Mallinckrodt, St. Louis, MO. Naloxone was purchased from Sigma-Aldrich (St. Louis, MO). All drugs and test compounds were dissolved in pyrogen-free isotonic saline (Baxter Healthcare, Deerfield, IL) and were administered to mice subcutaneously (sc).

Experimental Design and Statistical Analysis. To test for agonist properties, mice with predetermined tail immersion baseline, were injected sc with morphine (10 mg/kg; a dose that produces maximal antinociception) or the test compound at increasing doses and were reassessed for their tail immersion reaction time 20 min later. To test for antagonist properties, mice with predetermined tail immersion baseline, were injected sc with either naloxone (1 mg/kg; a dose that totally block the antinociception induce by 10 mg/kg morphine) or the test compound at various doses and 5 min later they were administered morphine (10 mg/kg; sc). Mice were reassessed for their tail immersion reaction time 20 min later. Effective dose-50 (ED_{50}) values were calculated using least-squares linear regression analysis followed by calculation of 95% confidence limits (95% CL) by the method of Bliss.[60]

Data are expressed as mean values ± SEM analysis of variance (ANOVA) followed by the post hoc "Student−Newman−Keuls" test were performed to assess significance using the Instat 3.0 software (GraphPad Software, San Diego, CA). $P < 0.05$ was considered significant.

Acknowledgment. We thank Dr. Lee-Yuan Liu-Chen at Temple University and Dr. Ping-Yee Law at the University of Minnesota for the generous gift of opioid receptor expressed CHO cell lines. We appreciate the generous help from Mallinckrodt, Inc., for the gift of naltrexone sample. The work was partially supported by PHS grants from NIH/NIDA, DA010770 (DES), DA007027 and DA000480 (WLD), and DA024022 (YZ). The content is solely the responsibility of the authors and does not necessarily represent the official views of the National Institute On Drug Abuse or the National Institutes of Health.

Supporting Information Available: Procheck results of three homology models and a table listing the HPLC retention times and mobile phase and method for analysis. This material is available free of charge via the Internet at http://pubs.acs.org.

References

(1) Zimmerman, D. M.; Leander, J. D. Selective opioid receptor agonists and antagonists: research tools and potential therapeutic agents. *J. Med. Chem.* **1990**, *33*, 895–902.
(2) Schmidhammer, H. Opioid Receptor Antagonists. *Prog. Med. Chem.* **1998**, *35*, 83–132.
(3) Snyder, S. H.; Pasternak, G. W. Historical Review: Opioid Receptors. *Trendss Pharmacol. Sci.* **2003**, *24* (4), 198–205.
(4) Fiellin, D. A.; Kleber, H.; Trumble-Hejduk, J. G.; McLellan, A. T.; Kosten, T. R. Consensus statement in office-based treatment of opioid dependence using buprenorphine. *J. Subst. Abuse Treat.* **2004**, *27*, 153–159.
(5) Gold, M. S.; Dackis, C. A.; Pottash, A. L.; Sternbach, H. H.; Annitto, W. J.; Martin, D.; Dackis, M. P. Naltrexone, opiate addiction, and endorphins. *Med. Res. Rev.* **1982**, *2* (3), 211–246.
(6) Gonzalez, J. P.; Brogden, R. N. Naltrexone. A review of its pharmacodynamic and pharmacokinetic properties and therapeutic efficacy in the management of opioid dependence. *Drugs* **1988**, *35*, 192–213.
(7) Schwyzer, R. ACTH: a short introductory review. *Ann. N.Y. Acad. Sci.* **1977**, *297*, 3–26.
(8) Portoghese, P. S.; Lipkowski, A. W.; Takemori, A. E. Binaltorphimine and nor-bionaltorphimine, potent and selective kappa opioid receptor antagonists. *Life Sci.* **1987**, *40*, 1287–1292.
(9) Jones, R. M.; Hjorth, S. A.; Schwartz, T. W.; Portoghese, P. S. Mutational evidence for a common kappa antagonist binding pocket in the wild-type kappa and mutant mu[K303E] opioid receptors. *J. Med. Chem.* **1998**, *41* (25), 4911–4914.
(10) Portoghese, P. S.; Sultana, M.; Nagase, H.; Takemori, A. E. Application of the message-address concept in the design of highly potent and selective non-peptide delta opioid receptor antagonist. *J. Med. Chem.* **1988**, *31*, 281–282.
(11) Schmidhammer, H.; Burkard, W. P.; Eggstin-Aeppli, L.; Smith, C. F. C. Synthesis and biological evaluation of 14-alkoxymorphinans. 2. (−)-*N*-(cyclopropymethyl)-4,14-dimethoxymorphinana-6-one, a selective mu opioid receptor antagonist. *J. Med. Chem.* **1989**, *32*, 418–421.
(12) Marki, A.; Monory, K.; Otvos, F.; Toth, G.; Krassnig, R.; Schmidhammer, H.; Traynor, J. R.; Roques, B. P.; Maldonado, R.; Borsodi, A. Mu-opioid receptor specific antagonist cyprodime: characterization by in vitro radioligand and [^{35}S]GTPgammaS binding assays. *Eur. J. Pharmacol.* **1999**, *383* (2), 209–214.

(13) Schmidhammer, H.; Jennewein, H. K.; Krassnig, R.; Traynor, J. R.; Patel, D.; Bell, K.; Froschauer, G.; Mattersberger, K.; Jachs-Ewinger, C.; Jura, P.; Fraser, G. L.; Kalinin, V. N. Synthesis and biological evaluation of 14-alkoxymorphinans. 11. 3-Hydroxycyprodime and analogues: opioid antagonist profile in comparison to cyprodime. *J. Med. Chem.* **1995**, *38* (16), 3071–3077.

(14) Schmidhammer, H.; Jennewein, H. K.; Smith, C. F. Synthesis and biological evaluation of 14-alkoxymorphinans. 11. 3-Hydroxycyprodime and analogues: opioid antagonist profile in comparison to cyprodime. *Arch. Pharm. (Weinheim).* **1991**, *324* (4), 209–211.

(15) Schmidhammer, H.; Smith, C. F.; Erlach, D.; Koch, M.; Krassnig, R.; Schwetz, W.; Wechner, C. Synthesis and biological evaluation of 14-alkoxymorphinans. 3. Extensive study on cyprodime-related compounds. *J. Med. Chem.* **1990**, *33* (4), 1200–1206.

(16) Schmidhammer, H.; Smith, C. F.; Erlach, D.; Koch, M.; Krassnig, R.; Schwetz, W.; Wechner, C. Cyprodime analogues: synthesis and pharmacological evaluation. *Prog. Clin. Biol. Res.* **1989**, *328*, 37–40.

(17) Spetea, M.; Schullner, F.; Moisa, R. C.; Berzetei-Gurske, I. P.; Schraml, B.; Dorfler, C.; Aceto, M. D.; Harris, L. S.; Coop, A.; Schmidhammer, H. Synthesis and biological evaluation of 14-alkoxymorphinans. 21. Novel 4-alkoxy and 14-phenylpropoxy derivatives of the mu opioid receptor antagonist cyprodime. *J. Med. Chem.* **2004**, *47* (12), 3242–3247.

(18) Lewis, J. W.; Smith, C. F. C.; McCarthy, P. S.; Walter, D.; Kobylecki, R. J.; Myers, M.; Haynes, A. S.; Lewis, C. J.; Waltham, K. New 14-aminomorphinones and codeinones. *NIDA Res. Monogr.* **1988**, *90*, 136–143.

(19) Portoghese, P. S.; Takemori, A. E. Affinity labels as probes for opioid receptor types and subtypes. *NIDA Res. Monogr.* **1986**, *69*, 157–168.

(20) Burke, T. F.; Woods, J. H.; Lewis, J. W.; Medzihradsky, F. Irreversible opioid antagonist effects of clocinnamox on opioid analgesia and mu receptor binding in mice. *J. Pharmacol. Exp. Ther.* **1994**, *271* (2), 715–721.

(21) Eguchi, M. Recent advances in selective opioid receptor agonists and antagonists. *Med. Res. Rev.* **2004**, *24* (2), 182–212.

(22) Pelton, J. T.; Kazmierski, W.; Gulya, K.; Yamamura, H. I.; Hruby, V. J. Design and synthesis of conformationally constrained somatostatin analogues with high potency and specificity for mu opioid receptors. *J. Med. Chem.* **1986**, *29*, 2370–2375.

(23) Gulya, K.; Pelton, J. T.; Hruby, V. J.; Yamamura, H. I. Cyclic somatostatin octapeptide analogues with high affinity and selectivity toward mu opioid receptors. *Life Sci.* **1986**, *38*, 2221–2230.

(24) Hawkins, K. N.; Knapp, R. J.; Lui, G. K.; Gulya, K.; Kazmierski, W.; Wan, Y. P.; Pelton, J. T.; Hruby, V. J.; Yamamura, H. I. [^{3}H]-[H-D-Phe-Cys-Tyr-D-Trp-Orn-Thr-Pen-Thr-NH2] ([3H]CTOP), a potent and highly selective peptide for mu opioid receptors in rat brain. *J. Pharmacol. Exp. Ther.* **1989**, *248* (1), 73–81.

(25) Kramer, T. H.; Shook, J. E.; Kazmierski, W.; Ayres, E. A.; Wire, W. S.; Hruby, V. J.; Burks, T. F. Novel peptidic mu opioid antagonists: pharmacologic characterization in vitro and in vivo. *J. Pharmacol. Exp. Ther.* **1989**, *249* (2), 544–551.

(26) Hruby, V. J.; Toth, G.; Gehrig, C. A.; Kao, L. F.; Knapp, R.; Lui, G. K.; Yamamura, H. I.; Kramer, T. H.; Davis, P.; Burks, T. F. Topographically designed analogues of [D-Pen, D-Pen5]enkephalin. *J. Med. Chem.* **1991**, *34* (6), 1823–1830.

(27) (a) Mulder, A. H.; Wardeh, G.; Hogenboom, F.; Kazmierski, W.; Hruby, V. J.; Schoffelmeer, A. N. Cyclic somatostatin analogues as potent antagonists at mu-, but not delta- and kappa-opioid receptors mediating presynaptic inhibition of neurotransmitter release in the brain. *Eur. J. Pharmacol.* **1991**, *205* (1), 1–6. (b) Abbruscato, T. J.; Thomas, S. A.; Hruby, V. J.; Davis, T. P. Blood−brain barrier permeability and bioavailability of a highly potent and mu-selective opioid receptor antagonist, CTAP: comparison with morphine. *J. Pharmacol. Exp. Ther.* **1997**, *280* (1), 402–409.

(28) Bonner, G. G.; Davis, P.; Stropova, D.; Edsall, S.; Yamamura, H. I.; Porreca, F.; Hruby, V. J. Opiate aromatic pharmacophore structure-activity relationships in CTAP analogues determined by topographical bias, two-dimensional NMR, and biological activity assays. *J. Med. Chem.* **2000**, *43* (4), 569–580.

(29) Okada, T.; Le Trong, I.; Fox, B. A.; Behnke, C. A.; Stenkamp, R. E.; Palczewski, K. X-Ray diffraction analysis of three-dimensional crystals of bovine rhodopsin obtained from mixed micelles. *J. Struct. Biol.* **2000**, *130* (1), 73–80.

(30) Teller, D. C.; Okada, T.; Behnke, C. A.; Palczewski, K.; Stenkamp, R. E. Advances in determination of a high-resolution three-dimensional structure of rhodopsin, a model of G-protein-coupled receptors (GPCRs). *Biochemistry* **2001**, *40* (26), 7761–7772.

(31) Salom, D.; Le Trong, I.; Pohl, E.; Ballesteros, J. A.; Stenkamp, R. E.; Palczewski, K.; Lodowski, D. T. Improvements in G protein-coupled receptor purification yield light stable rhodopsin crystals. *J. Struct. Biol.* **2006**, *156* (3), 497–504.

(32) Salom, D.; Lodowski, D. T.; Stenkamp, R. E.; Le Trong, I.; Golczak, M.; Jastrzebska, B.; Harris, T.; Ballesteros, J. A.; Palczewski, K. Crystal structure of a photoactivated deprotonated intermediate of rhodopsin. *Proc. Natl. Acad. Sci. U.S.A.* **2006**, *103* (44), 16123–16128.

(33) Park, J. H.; Scheerer, P.; Hofmann, K. P.; Choe, H. W.; Ernst, O. P. Crystal structure of the ligand-free G-protein-coupled receptor opsin. *Nature.* **2008**, *454*, 183–187.

(34) Rasmussen, S. G.; Choi, H. J.; Rosenbaum, D. M.; Kobilka, T. S.; Thian, F. S.; Edwards, P. C.; Burghammer, M.; Ratnala, V. R.; Sanishvili, R.; Fischetti, R. F.; Schertler, G. F.; Weis, W. I.; Kobilka, B. K. Crystal structure of the human beta(2) adrenergic G-protein-coupled receptor. *Nature* **2007**, *450* (7168), 383–387.

(35) Rosenbaum, D. M.; Cherezov, V.; Hanson, M. A.; Rasmussen, S. G.; Thian, F. S.; Kobilka, T. S.; Choi, H.-J.; Yao, X.-J.; Weis, W. I.; Stevens, R. C.; Kobilka, B. K. GPCR Engineering Yields High-Resolution Structural Insights into 2 Adrenergic Receptor Function. *Science,* **2007**, *318* (5854), 1266–1273.

(36) Cherezov, V.; Rosenbaum, D. M.; Hanson, M. A.; Rasmussen, S. G.; Thian, F. S.; Kobilka, T. S.; Choi, H.-J.; Kuhn, P.; Weis, W. I.; Kobilka, B. K.; Stevens, R. C. High-Resolution Crystal Structure of an Engineered Human 2-Adrenergic G Protein-Coupled Receptor. *Science* **2007**, *318* (5854), 1258–1265.

(37) Hanson, M. A.; Cherezov, V.; Griffith, M. T.; Roth, C. B.; Jaakola, V. P.; Chien, E. Y.; Velasquez, J.; Kuhn, P.; Stevens, R. C. A specific cholesterol binding site is established by the 2.8 Å structure of the human beta2-adrenergic receptor. *Structure* **2008**, *16* (6), 897–905.

(38) Warne, T.; Serrano-Vega, M. J.; Baker, J. G.; Moukhametzianov, R.; Edwards, P. C.; Henderson, R.; Leslie, A. G.; Tate, C. G.; Schertler, G. F. Structure of a beta(1)-adrenergic G-protein-coupled receptor. *Nature* **2008**, *454* (7203), 486–491.

(39) Zhang, Y.; Sham, Y. Y.; Rajamani, R.; Gao, J. L.; Portoghese, P. S. Homology Modeling of the Mu Opioid Receptor Built in a Complete Membrane−Aqueous System. *ChemBioChem* **2005**, *6*, 853–859.

(40) Metzger, T. G.; Paterlini, M. G.; Ferguson, D. M.; Portoghese, P. S. Investigation of the selectivity of oxymorphone- and naltrexone-derived ligands via site-directed mutagenesis of opioid receptors: exploring the "address" recognition locus. *J. Med. Chem.* **2001**, *44*, 857–862.

(41) Ulens, C.; Baker, L.; Ratka, A.; Waumans, D.; Tytgat, J. Morphine-6beta-glucuronide and morphine-3-glucuronide, opioid receptor agonists with different potencies. *Biochem. Pharmacol.* **2001**, *62*, 1273–1282.

(42) Fowler, C. B.; Pogozheva, I. D.; LeVine, H., III.; Mosberg, H. I. Refinement of a homology model of the mu-opioid receptor using distance constraints from intrinsic and engineered zinc-binding sites. *Biochemistry* **2004**, *43*, 8700–8710.

(43) Xue, J.-C.; Chen, C.; Zhu, J.; Kunapuli, S. P.; de Riel, J. K.; Yu, L.; Liu-Chen, L.-Y. The third extracellular loop of the mu opioid receptor is important for agonist selectivity. *J. Biol. Chem.* **1995**, *270*, 12977–12979.

(44) Bonner, G.; Meng, F.; Akil, H. Selectivity of mu-opioid receptor determined by interfacial residues near the third extracellular loop. *Eur. J. Pharmacol.* **2000**, *403*, 37–44.

(45) Zhu, J.; Xue, J.-C.; Law, P.-Y.; Claude, P. A.; Luo, L.-Y.; Yin, J.; Chen, C.; Liu-Chen, L.-Y. The region in the mu opioid receptor conferring selectivity for sufentanil over the delta receptor is different from that over the kappa receptor. *FEBS Lett.* **1996**, *384*, 198–202.

(46) Xu, W.; Li, J.; Chen, C.; Huang, P.; Weinstein, H.; Javitch, J. A.; Shi, L.; de Riel, J. K.; Liu-Chen, L. Y. Comparison of the amino acid residues in the sixth transmembrane domains accessible in the binding-site crevices of mu, delta, and kappa opioid receptors. *Biochemistry* **2001**, *40*, 8018–8029.

(47) Law, P. Y.; Wong, Y. H.; Loh, H. H. Mutational analysis of the structure and function of opioid receptors. *Biopolymers* **1999**, *51* (6), 440–455.

(48) Xu, H.; Lu, Y. F.; Partilla, J. S.; Zheng, Q. X.; Wang, J. B.; Brine, G. A.; Carroll, F. I.; Rice, K. C.; Chen, K. X.; Chi, Z. Q.; Rothman, R. B. Opioid peptide receptor studies, 11: involvement of Tyr148, Trp318 and His319 of the rat μ-opioid receptor in binding of μ-selective ligands. *Synapse (New York)* **1999**, *32* (1), 23–28.

(49) Griffin, J. F.; Larson, D. L.; Portoghese, P. S. Crystal structures of alpha- and beta-funaltrexamine: conformational requirement of the fumaramate moiety in the irreversible blockage of mu opioid receptors. *J. Med. Chem.* **1986**, *29* (5), 778–783.

(50) Sayre, L. M.; Portoghese, P. S. Stereospecific synthesis of the 6α- and 6β-amino derivatives of naltrexone and oxymorphone. *J. Org. Chem.* **1980**, *45*, 3366–3368.

(51) Keen, M. Testing models of agonism for G protein-coupled receptors. *Trends Pharmacol. Sci.* **1991**, *12* (10), 371–374.

(52) Selley, D. E.; Sim, L. J.; Xiao, R.; Liu, Q.; Childers, S. R. Mu-Opioid receptor-stimulated guanosine-5′-*O*-(gamma-thio)-triphosphate binding in rat thalamus and cultured cell lines: signal transduction mechanisms underlying agonist efficacy. *Mol. Pharmacol.* **1997**, *51* (1), 87–96.

(53) Selley, D. E.; Liu, Q.; Childers, S. R. Signal transduction correlates of mu opioid agonist intrinsic efficacy: receptor-stimulated [35S]GTPγS binding in mMOR-CHO cells and rat thalamus. *J. Pharmacol. Exp. Ther.* **1998**, *285*, 496–505.
(54) Morgan, D.; Cook, C. D.; Picker, M. J. Sensitivity to the discriminative stimulus and antinociceptive effects of mu opioids: role of strain of rat, stimulus intensity, and intrinsic efficacy at the mu opioid receptor. *J. Pharmacol. Exp. Ther.* **1999**, *289* (2), 965–975.
(55) Morgan, D.; Cook, C. D.; Smith, M. A.; Picker, M. J. An examination of the interactions between the antinociceptive effects of morphine and various mu-opioids: the role of intrinsic efficacy and stimulus intensity. *Anesth. Analg.* **1999**, *88* (2), 407–413.
(56) To further verify the role of Tyr210 and Trp318 in the binding of two leads to MOR, we conducted an initial site-directed mutagenesis study with CHO cells transiently transfected with the wild type and mutant MORs (Y210A and W318A). Naltrexone was used as control ligand and its binding affinity did not change much in both wild-type (wt) and mutant MORs (IC_{50} values were 3.90 ± 2.96 nM (wt), 0.95 ± 0.49 nM (Y210A), and 10.35 ± 1.64 nM (W318A), respectively). Both compound **6** and **9** bound to the Y210A mutant MOR with comparable affinities (IC_{50}, **6**, 1.61± 0.17 nM; **9**, 3.31 ± 1.71 nM) as to the wild-type MOR (IC_{50}, **6**, 2.29 ± 0.15 nM; **9**, 5.42 ± 0.70 nM), whereas their affinities were dramatically lower in binding to the W318A mutant (IC_{50}, **6**, >1000 nM; **9**, >1000 nM). We will revisit these studies with wider concentration range in order to define the IC_{50} and K_i values for this mutant. These results indicate that these two leads could recognize an "address" locus with potential hydrogen bonding property in the MOR, which could confer their selectivity for the MOR over the DOR and KOR.
(57) *InsightII User Guide*; MSI: San Diego, October 1995.
(58) Coderre, T. J.; Rollman, G. B. Naloxone hyperalgesia and stress-induced analgesia in rats. *Life Sci.* **1983**, *32* (18), 2139–2146.
(59) Harris, L. S.; Pierson, A. K. Some narcotic antagonists in the benzomorphan series. *J. Pharmacol. Exp. Ther.* **1964**, *143*, 141–148.
(60) Bliss, C. I. Statistics in Biology; McGraw-Hill: New York, 1967; p 439.
(61) Xhaard, H.; Nyrönen, T.; Rantanen, V. V.; Ruuskanen, J. O.; Laurila, J.; Salminen, T.; Scheinin, M.; Johnson, M. S. Model structures of α-2 adrenoceptors in complex with automatically docked antagonist ligands raise the possibility of interactions dissimilar from agonist ligands. *J. Struct. Biol.* **2005**, *150*, 126–143.

JM801272C